NASA TECHNICAL MEMORANDUM

NASA TM X-3172

NASA TM X-3172

METHOD OF PREDICTING RADIATION HEAT TRANSFER IN TURBINE-COOLING TEST FACILITIES

Herbert J. Gladden and Curt H. Liebert

Lewis Research Center

Cleveland, Ohio 44135

NATIONAL AERONAUTICS AND SPACE ADMINISTRATION • WASHINGTON, D. C. • JANUARY 1975

1. Report No. NASA TM X-3172	2. Government Accession No.	3. Recipient's Catalog No.
4. Title and Subtitle METHOD OF PREDICTING RADIATION HEAT TRANSFER IN TURBINE-COOLING TEST FACILITIES		5. Report Date January 1975 6. Performing Organization Code
7. Author(s) Herbert J. Gladden and Curt H. Liebert		8. Performing Organization Report No. E-8110 10. Work Unit No. 505-04
9. Performing Organization Name and Address Lewis Research Center National Aeronautics and Space Administration Cleveland, Ohio 44135		11. Contract or Grant No. 13. Type of Report and Period Covered Technical Memorandum
12. Sponsoring Agency Name and Address National Aeronautics and Space Administration Washington, D.C. 20546		14. Sponsoring Agency Code

15. Supplementary Notes

16. Abstract

A method is presented for calculating the average net radiation heat flux to turbine vanes and blades. The net radiation heat flux at a vane leading edge calculated by this method was compared with heat flux values independently determined from experimental tests on a vane in a cascade. The spectral emissivities of the turbine vane and the cascade wall were also measured.

17. Key Words (Suggested by Author(s))

Heat transfer
Radiation
View factor
Emissivity measurement
Hot-gas cascade

18. Distribution Statement

Unclassified - unlimited
STAR category 34 (rev.)

19. Security Classif. (of this report)	20. Security Classif. (of this page)	21. No. of Pages	22. Price*
Unclassified	Unclassified	21	$3.00

* For sale by the National Technical Information Service, Springfield, Virginia 22151

METHOD OF PREDICTING RADIATION HEAT TRANSFER IN TURBINE-COOLING TEST FACILITIES

by Herbert J. Gladden and Curt H. Liebert

Lewis Research Center

SUMMARY

A method is presented for calculating the average net radiation heat flux to turbine vanes and blades. The heat flux at a vane leading edge calculated by this method was compared with heat flux values independently obtained from experimental tests with solid vanes in a cascade. The analytical method predicted the experimental heat flux data within ±20 percent. The spectral emissivities of the vane and cascade wall materials, required for the calculation, were also measured.

INTRODUCTION

An analytical method for calculating the average net radiation heat flux on gas turbine vanes and blades was developed and then evaluated by comparing the predicted values with limited experimental radiation heat flux data. There are situations where the radiation components of heat transfer are significant and should be considered in the analysis of turbine cooling performance. For instance, the net radiation heat flux in advanced high-pressure engines could be as much as 30 percent of the total heat flux to the first-stage vane row. In practice, the net radiation heat flux is frequently assumed to be an arbitrary percentage increase over the calculated convective heat flux. This approach, however, can be misleading. Under certain circumstances, net radiation heat flux may be directed either to or from the vane surface. Included in these circumstances might be (1) a cool turbine vane surface absorbing energy from a high-emittance, high-temperature gas flame source; or (2) a hot turbine vane surface emitting to a cool surrounding wall.

A simple analytical model that uses existing techniques and that can account for the net and individual components of radiation is needed, particularly as turbine inlet temperature and pressure increase. This report presents an analytical method of predicting

the net radiation heat flux to gas turbine vanes and blades and provides experimental verification of the analysis. It would be desirable to verify, individually, the influence of all the components comprising the net radiation heat flux; however, the available data did not permit this completeness. The experimental net flux data used for verification were from reference 1 for solid, uncooled vanes in a four-vane cascade tested at a gas pressure of 3 atmospheres and a range of gas temperatures from 800 to 1100 K. In addition, the combustor was located relatively far upstream of the vane row such that flame radiation to the vane would be less than would be expected in an actual engine application.

Emissivity data on the vane and the cascade wall specimens were also obtained during separate experiments. These data were obtained at specimen temperatures of 300 to 1088 K and at wavelengths of 1 to 14.2 micrometers.

CALCULATION PROCEDURE

The main purpose of this study was to develop a method for calculating the average net radiation heat flux on turbine vanes and blades in engine and cascade facilities. This method uses the general engineering relations presented in reference 2 to evaluate the individual radiation components comprising the net radiation heat flux. A secondary purpose of the study was to compare the predicted net radiation heat flux values with experimental net radiation heat flux data from the leading edge of J-75 size turbine vanes tested in the cascade facility of reference 1. A side view of this facility is shown in figure 1. However, it is important to recognize that the comparison presented is only a limited verification of the accuracy of this method. In the cascade tests the component of the radiation heat flux from the vane to the cascade walls predominated. This test environment did not simulate that expected in an actual engine, in which the flame radiation to a vane would probably predominate. The experimental data available for comparison were obtained at gas temperatures of 800 to 1100 K and a gas pressure of 3 atmospheres.

Net Calculated Radiation Heat Flux

The net radiation heat flux from (or to) a given turbine vane (or blade) surface $q_{r,net}$ was taken as the heat flux emitted by the vane surface q_v, minus the absorbed heat flux emitted from the primary zone (flame zone region) of the combustor q_f, minus the absorbed heat flux emitted by the combustor secondary zone (dilution region) and the intervening gas volume (combustion gas region) positioned between the combustor exit and the vane row inlet q_g, minus the absorbed heat flux emitted by the surrounding

walls q_w. This statement is expressed as

$$q_{r,net} = q_v - q_f - q_g - q_w \tag{1}$$

The symbols are defined in appendix A. The net radiation exchange between adjacent vanes was assumed to be zero because all vanes were at essentially the same temperature. The reflective components of heat flux were assumed to be negligible because of the attenuating effect of the intervening gas and the low values of vane and cascade wall reflectivity involved. A further simplification was made by assuming that the emitting-absorbing combustion gas was isothermal.

Heat flux emitted by vane surface. - The radiation heat flux emitted by a turbine vane surface was determined by the vane surface temperature, the vane surface total hemispherical emissivity evaluated at the surface temperature, the associated view factor from the vane to the surrounding walls, and the equation

$$q_v = F_{v-w}\epsilon_v\sigma T_v^4 \tag{2}$$

The determination of the total hemispherical emissivity of the oxidized vane material (MAR M 302) ϵ_v and the diffuse view factor F_{v-w} is discussed in subsequent sections.

Heat flux emitted by primary zone of combustor. - The radiation heat flux from the primary (flame) zone which is transmitted through the secondary (dilution) zone and combustion gas volume region and absorbed per vane unit area was calculated by

$$q_f = \left(F_{v-f}\epsilon_f\sigma T_f^4\right)\alpha_v\tau_g \tag{3}$$

The primary zone was considered as that part of the combustor which operates at a stoichiometric fuel-air ratio and temperature; the secondary zone was taken as the combustor dilution region. The combustion gas was defined as that gas which occupies the volume between the end of the combustor and the vane row inlet. In the primary zone the major source and strength of radiation energy was carbon dioxide (CO_2), water vapor (H_2O), and soot. The experimental data of reference 3 indicate that the primary-zone emittance[1] ϵ_f was approximately 0.2 for the 3-atmosphere gas pressure of the reference 1 data. The method for calculating the transmittance τ_g of the secondary-zone and combustion gas region is discussed in the section Combustion Gas Emittance and Transmittance.

[1]Following the nomenclature of reference 2, the -ivity ending will be used throughout for the radiative properties of opaque materials (solids) and the -ance ending will be reserved for the radiative properties of gases.

The vane total hemispherical absorptivity α_v was assumed to equal the vane total hemispherical emissivity. This assumption is reasonable because, as is shown in appendix B, the spectral normal emissivity of the vane material (oxidized MAR M 302) varies little with wavelength.

Heat flux emitted by secondary zone and combustion gas. - The secondary-zone radiation heat flux absorbed per vane unit area was lumped with the combustion gas radiation heat flux and written as

$$q_g = \left(\epsilon_g \sigma T_g^4\right)\alpha_v \tag{4}$$

Because the carbon particles are rapidly burned up in the secondary zone, the emittance of the secondary-zone and combustion gas region was assumed to be dependent only on CO_2 and H_2O constituents. The total hemispherical emittance of these constituents was calculated by using Hottel's data and was based on the mean beam length (discussed later) of an optically thick gray gas (ref. 2). The gas temperature was taken as the average static temperature of the gas volume.

Heat flux emitted by surrounding walls. - The radiation heat flux from the surrounding walls, which is absorbed per unit area of the vane surface, was calculated from the relation

$$q_w = \left(F_{v-w}\epsilon_w \sigma T_w^4\right)\alpha_v \tau_g \tag{5}$$

where ϵ_w is the wall emissivity evaluated at the wall temperature and τ_g is the transmittance of the gas (discussed later). A nominal value was used herein for the cascade wall temperature T_w which neglects the presence of the liner in the transition section and considers only the temperature of the water-cooled walls of the test section since the view factor from the vane to the liner was small (<0.05). The gas-side temperature of the cascade walls was determined from temperature data measured on the water side.

Total Hemispherical Emissivity

The total normal emissivity of the vane material (oxidized MAR M 302) and the cascade wall material (plasma-sprayed aluminum oxide (Al_2O_3)) was based on the spectral normal emissivity data found experimentally by using spectroscopic equipment. This procedure is discussed in detail in appendix B. The total hemispherical emissivity required in the calculation procedure was assumed to be equal to the total normal emissivity. This assumption was reasonable because the vane surfaces and the cascade wall surfaces were oxidized and were not optically smooth.

Combustion Gas Emittance and Transmittance

The combustion gas mixture was composed of water vapor and carbon dioxide. The emittance of this mixture was evaluated with the following relation (ref. 2):

$$\epsilon_g = C_{CO_2}\epsilon_{CO_2} + C_{H_2O}\epsilon_{H_2O} - \Delta\epsilon' \tag{6}$$

The values of the parameters in equation (6) were obtained from figures 17-11 to 17-15 of reference 2. These values are a function of the partial pressure of the water vapor and carbon dioxide, the mean beam length (gas-to-surface exchange) of an optically thick gas, and the static gas temperature. This mean beam length (an average gas path length) is expressed as

$$L_e = 3.6\,\frac{\text{Volume of gas}}{\text{Surface area of gas volume}} \tag{7}$$

As discussed in reference 2, the mean beam length is the required radius of a gas hemisphere that radiates a flux to the center of its base equal to the average flux radiated to the area of interest by the actual volume of gas. For proper use of equations (6) and (7), the enclosure boundary should be essentially nonreflecting.

The transmittance of the combustion gas mixture is related to the absorptance by

$$\tau_g = 1 - \alpha_g \tag{8}$$

The absorptance of the gas was evaluated with the following relation (ref. 2):

$$\alpha_g = C_{CO_2}\epsilon^{+}_{CO_2}\left[\frac{T_g}{T_{w(\text{or } f)}}\right]^{0.65} + C_{H_2O}\epsilon^{+}_{H_2O}\left[\frac{T_g}{T_{w(\text{or } f)}}\right]^{0.45} - \Delta\alpha' \tag{9}$$

where $\epsilon^{+}_{H_2O}$, $\epsilon^{+}_{CO_2}$, and $\Delta\alpha'$ were obtained from figures 17-11 to 17-15 of reference 2 but were evaluated at T_w or T_f. As discussed in reference 2, $\epsilon^{+}_{CO_2}$ and $\epsilon^{+}_{H_2O}$ were evaluated by using the geometric mean beam length (surface-to-surface exchange), which is a mean value of the path length of gas between the vane and the surrounding walls or the primary-zone flame. For convenience, the geometric mean beam length was assumed to equal the mean beam length. This assumption is reasonable because the volume of gas viewed by a given vane surface (and therefore considered for the calculation of the path length L_e) is mostly contained by the tunnel walls. The cascade geometry associated with evaluating L_e for a given dA_v is shown in figure 2(a). The

volumes and areas were determined from a 10-times-size layout of the cascade sections of reference 1. Some additional details of the cascade geometry are given in appendix C.

Diffuse View Factors

In general, a given vane surface element (ref. 1) will view all of a wall within that surface element's hemispherical viewing field, minus that part of a wall which is blocked from view by an adjacent vane. That is, the view factor F_{v-w} (eqs. (2) and (5)) is always unity minus the view factor from the surface element to that part of a wall which cannot be "seen" by the surface element. This relation is expressed as

$$F_{v-w} = 1 - F^* \tag{10}$$

A typical representation of this idea, as applied to the cascade, is shown schematically in figure 2(b), where F^* pertains to those regions within the dashed lines. Typical leading-edge suction surface and pressure surface vane-to-cascade-wall view factors (fig. 3) were calculated by using a differential line source at an angle φ (ref. 4). The view factor from the vane to the primary zone of the combustor used herein was represented by a ratio of differential vane surface area to an annular flame surface area (calculated as 0.0069).

The calculated view factors and mean beam lengths for the three regions of each vane of reference 1 are presented in table I.

Net Radiation Heat Flux from Reference 1 Data

The experimental net radiation heat flux values were obtained from solid vanes in a four-vane cascade (ref. 1). A heat balance on an element of a vane shows that the net radiation component of heat transfer was the difference between the gas-side convection heat flux and the conduction losses

$$q_{r,\,net,\,exp} = q_{conv} - q_{cond} \tag{11}$$

The convection component was defined as follows:

$$q_{conv} = h_{g,\,calc}(T_{ge} - T_{wm}) \tag{12}$$

For the leading-edge region, $h_{g,\,calc}$ was calculated by equation (13), which is typically used to find the local gas-side heat transfer coefficient around the leading edge of a turbine vane. The effective gas temperature T_{ge} was calculated from the measured inlet total temperature and a turbulent recovery factor; the vane wall temperature T_{wm} was measured.

$$Nu = 1.14\,Re^{0.5}Pr^{0.4}\left(1 - \left|\frac{\theta}{90}\right|^{3}\right) \tag{13}$$

The conduction component of heat flux was the sum of the chordwise and spanwise terms

$$q_{cond} = \sum k\frac{dT_{wm}}{dx} \tag{14}$$

Temperature products were determined from chordwise and spanwise experimental temperature profiles.

COMPARISON OF PREDICTED AND EXPERIMENTAL DATA

The average net radiation heat flux from the leading edge of turbine vanes as determined from the experimental data of reference 1 (using eq. (11)) was compared with that calculated by equation (1). This comparison is shown in figure 4. The magnitude of $q_{r,\,net}$ and of each term of equation (1) is shown in table II. The heat flux from three regions of the leading edge is presented. These regions are (1) the stagnation region (thermocouple 1 of insert to fig. 4), (2) the suction surface (thermocouple 2 of insert to fig. 4), and (3) the pressure surface (thermocouple 3 of insert to fig. 4). Table II shows that the radiation heat flux from the vane surface was predominant. The sum of the remaining heat flux terms (flame, combustion gas, and cascade walls) was between 20 and 30 percent of that from the vane surface.

The dashed lines in figure 4 show that equation (1) predicts the majority of the experimental data within ±20 percent. This is considered as good agreement, since it has been estimated (ref. 1) that the net experimental heat flux calculated by equation (11) could be in error by ±20 percent because of the correlation spread and the measurement error. In addition, the predicted data could be in error by about ±10 percent because of the error associated with the measured spectral emissivities (±3 percent) and the uncertainty associated with the simplifying assumptions.

Because very little information was available concerning the vane material of reference 1 (oxidized MAR M 302), emissivity data for this material were measured; the results are presented in appendix B.

CONCLUDING REMARKS

A method of calculating the net radiation heat flux to turbine vanes or blades by using available engineering relations was developed. As a partial check the method was applied to some experimental data which were dominated by the radiation heat flux emitted by the solid vanes. Data were not available to check cases where the flame or the combustion gas radiation heat fluxes were dominant. For the case studied the analytical method predicted the experimental data within ±20 percent.

Lewis Research Center,
National Aeronautics and Space Administration,
Cleveland, Ohio, October 18, 1974,
505-04.

APPENDIX A

SYMBOLS

A	area
b_1	constant in eq. (B1), 1.2864×10^{-15} W cm^{-2} μm^{-1} K^{-5}
C	pressure correction coefficient in eqs. (6) and (9)
F	diffuse view factor
h	heat transfer coefficient
k	thermal conductivity
L_e	mean beam length
Nu	Nusselt number
Pr	Prandtl number
q	heat flux per unit area
Re	Reynolds number
T	temperature
W_λ	spectral intensity of a black body
$W_{\lambda m}$	maximum spectral intensity of a black body
x	distance
α	total hemispherical absorptivity (absorptance)
$\Delta\alpha', \Delta\epsilon'$	correction for spectral overlap
ϵ	total hemispherical emissivity (emittance)
$\epsilon_{t,n}$	total normal emissivity
ϵ_λ	spectral normal emissivity
θ	angle measured from stagnation point
λ	wavelength
σ	Stefan-Boltzmann constant, 5.669×10^{-12} W cm^{-2} K^{-4}
τ	transmittance
φ	angle between plane of line source and rectangle (figs. 2 and 3)

Subscripts:

CO_2	carbon dioxide

calc	calculated
cond	conduction
conv	convection
exp	experimental
f	flame
g	gas
ge	effective gas
H_2O	water vapor
net	net
r	radiation
s	specimen
v	vane surface
v-f	from vane surface to flame
v-w	from vane surface to cascade wall
w	cascade wall
wm	measured vane surface

Superscripts:

*	associated with diffuse view factor from a given vane surface element to that part of the cascade wall blocked from view by adjacent vane (eq. (10))
+	quantities defined in eq. (9)

APPENDIX B

TOTAL HEMISPHERICAL EMISSIVITY OF CASCADE WALL AND VANE MATERIAL

The total normal emissivity can be found from the following equation:

$$\epsilon_{t,N} = \frac{b_1 T_s}{\sigma} \int_0^\infty \epsilon_\lambda \frac{W_\lambda}{W_{\lambda m}} d\lambda \tag{B1}$$

where the normal spectral emissivity ϵ_λ is usually experimentally determined. Values of $W_\lambda/W_{\lambda m}$ were obtained from reference 5, where the product $\epsilon_\lambda(W_\lambda/W_{\lambda m})$ is a function of wavelength for various surface temperatures T_s. The total normal emissivity was calculated from the product of $b_1 T_s/\sigma$ and the integrated terms.

Figure 5 shows the measured normal spectral emissivity of the cascade wall material (Al_2O_3) coated onto stainless steel and the vane material (oxidized MAR M 302) for wavelengths of 1 to 14.2 micrometers. The emissivity values were obtained by using a recording infrared spectrophotometer (ref. 6). At the temperatures studied (300, 800, and 1080 K) the normal spectral emissivity varied little (±3 percent) with temperature. The dashed lines indicate values of data taken from reference 7 which were also needed to calculate $\epsilon_{t,N}$. The total normal emissivity values so obtained were assumed to equal the total hemispherical emissivity.

The Al_2O_3-insulated cascade walls of reference 1 were covered with a coating of soot during operation. Thus, the radiative properties of the cascade walls could depend on the properties of both the layer of soot and the Al_2O_3 coating. (The Al_2O_3 coating is opaque, and so the radiative properties of the steel walls will not affect the composite emissivity.) The ϵ_λ of the soot-Al_2O_3 composite could not be measured because it was difficult to obtain a sample of the composite during cascade operation. However, because the total normal emissivity of both Al_2O_3 and rough carbon samples (ref. 8) is about 0.85 at cascade wall operation temperatures (360 to 470 K), the emissivity of the composite of the two materials was also taken as 0.85.

The soot was rapidly oxidized at the vane testing temperatures of 800 to 1100 K (ref. 9). The vane emissivity, therefore, is the composite emissivities of MAR M 302 alloy and a thin layer of oxide. The spectral emissivity of the alloy composite (fig. 5) varied from about 0.78 to 0.97. Evaluating the total normal emissivity $\epsilon_{t,N}$ at a composite temperature of 800 to 1000 K resulted in a value of 0.85±0.02.

Because the total normal emissivities of both the vane and the tunnel walls were about 0.85, the assumptions of negligible vane-to-vane and vane-to-cascade-wall reflectivity previously discussed are reasonable.

For a gray surface, the total hemispherical absorptivity equals the total hemispherical emissivity. The spectral emissivity of the vane (fig. 5) varies little with wavelength and thus the assumption of $\alpha_v = \epsilon_v$ for the vane surface is justifiable.

APPENDIX C

EXPERIMENTAL APPARATUS OF REFERENCE 1

A four-vane, five-flow-channel cascade was used in reference 1 to obtain the experimental average net radiation heat flux data presented herein. A detailed description of this facility is given in references 1 and 10. Briefly, the facility consisted of an inlet section, a burner section, a transition section, a test section, and an exit section, as shown schematically in figure 1. The test and exit section walls were water cooled and insulated on the gas side by plasma-sprayed Al_2O_3 (0.5 mm thick). The transition section had an Al_2O_3-sprayed liner between the water-cooled walls and the hot gas. The test section was a 23° annular sector of a J-75 vane row and contained four solid, noncooled vanes. These vanes (cast MAR M 302) had a span of 9.78 centimeters and a chord of 6.28 centimeters. A cross-sectional schematic of the test section is shown in figure 6. The central vanes were considered the test vanes and contained the majority of the thermocouples. The outer two vanes completed the flow channels for the test vanes and also served as radiation shields between the test vanes and the water-cooled cascade walls.

The vanes were tested at combustion gas temperatures from 810 to 1140 K and a gas pressure of about 3 atmospheres, which corresponds to an inlet gas Reynolds number range of 4×10^4 to 6×10^4. The temperature of the cascade walls (gas side) was determined from the coolant-side temperature measurements to be 360 to 470 K.

REFERENCES

1. Gladden, Herbert J.; Hippensteele, Steven A.; Hickel, Robert O.; and Dengler, Robert P.: Radiation Heat Transfer Characteristics of Turbine Vane Airfoils in a Water-Cooled Cascade. NASA TM X-2203, 1971.

2. Siegel, Robert; and Howell, John R.: Thermal Radiation Heat Transfer. McGraw-Hill Book Co., Inc., 1972.

3. Norgren, Carl T.: Determination of Primary-Zone Smoke Concentrations from Spectral Radiance Measurements in Gas Turbine Combustors. NASA TN D-6410, 1971.

4. Wiebelt, John A.: Engineering Radiation Heat Transfer. Holt, Rinehart, and Winston, Inc., 1966.

5. Harrison, Thomas R.: Radiation Pyrometry and its Underlying Principles of Radiant Heat Transfer. John Wiley & Sons, Inc., 1960.

6. Liebert, Curt H.: Spectral Emittance of Aluminum Oxide and Zinc Oxide on Opaque Substrates. NASA TN D-3155, 1974.

7. Touloukian, Y. S., ed.: Thermophysical Properties of Matter. Vol. 8, The Macmillan Co., 1972.

8. Svet, Darii I.: Thermal Radiation; Metals, Semiconductors, Ceramics, Partly Transparent Bodies and Films. Consultants Bureau, 1965.

9. Liebert, Curt H.; and Hibbard, Robert R.: Spectral Emittance of Soot. NASA TN D-5647, 1970.

10. Calvert, Howard F.; Cochran, Reeves P.; Dengler, Robert P.; Hickel, Robert O.; and Norris, James W.: Turbine Cooling Research Facility. NASA TM X-1927, 1970.

TABLE I. - VIEW FACTORS AND MEAN BEAM LENGTHS FOR SELECTED AREAS OF FOUR TURBINE VANES IN A CASCADE

Region	View factor, F_{v-w}, and mean beam length, L_e	Vane			
		1	2	3	4
Leading-edge, stagnation region	F_{v-w}	1.0	1.0	1.0	1.0
	L_e, m (ft)	0.183 (0.6)	0.183 (0.6)	0.183 (0.6)	0.183 (0.6)
Leading-edge, suction-surface region (thermocouple 2, fig. 4)	F_{v-w}	0.929	0.914	0.890	1.0
	L_e, m (ft)	0.183 (0.599)	0.183 (0.602)	0.184 (0.603)	0.185 (0.606)
Leading-edge, pressure-surface region (thermocouple 3, fig. 4)	F_{v-w}	1.0	0.883	0.904	0.923
	L_e, m (ft)	0.184 (0.605)	0.184 (0.604)	0.183 (0.601)	0.183 (0.599)

TABLE II. - CALCULATED NET RADIATION HEAT FLUX DATA BASED ON REFERENCE 1 TEST DATA

$[q_{r,net} = q_v - q_f - q_g - q_w]$

Run	Vane								
	2	3	Flame heat flux, q_f, W/m^2	2	3	2	3	2	3
	Vane surface heat flux, q_v, W/m^2			Gas heat flux, q_g, W/m^2		Cascade wall heat flux, q_w, W/m^2		Net heat flux, $q_{r,net}$, W/m^2	
Leading-edge, stagnation region									
1	19 550	19 000	1760	2 610	2 610	750	750	16 200	15 650
2	33 610	33 750	↓	4 960	4 960	715	715	27 950	28 080
3	------	52 650		8 080	8 080	1216	1216	------	43 380
4	------	77 450		12 050	12 050	1173	1173	------	64 250
Leading-edge, suction-surface region									
1	17 570	16 860	1245	2 610	2 610	687	668	14 290	13 600
2	30 600	29 900	↓	4 960	4 960	652	637	24 980	24 300
3	46 700	46 670		8 080	8 080	1110	1080	37 480	37 500
4	70 700	68 650		12 050	12 050	1070	1043	57 600	55 600
Leading-edge, pressure-surface region									
1	16 660	------	1245	2 610	------	662	----	13 710	------
2	29 530	------	↓	4 960	------	631	----	23 950	------
3	45 100	------		8 080	------	1070	----	35 950	------
4	68 400	------		12 050	------	1036	----	55 300	------

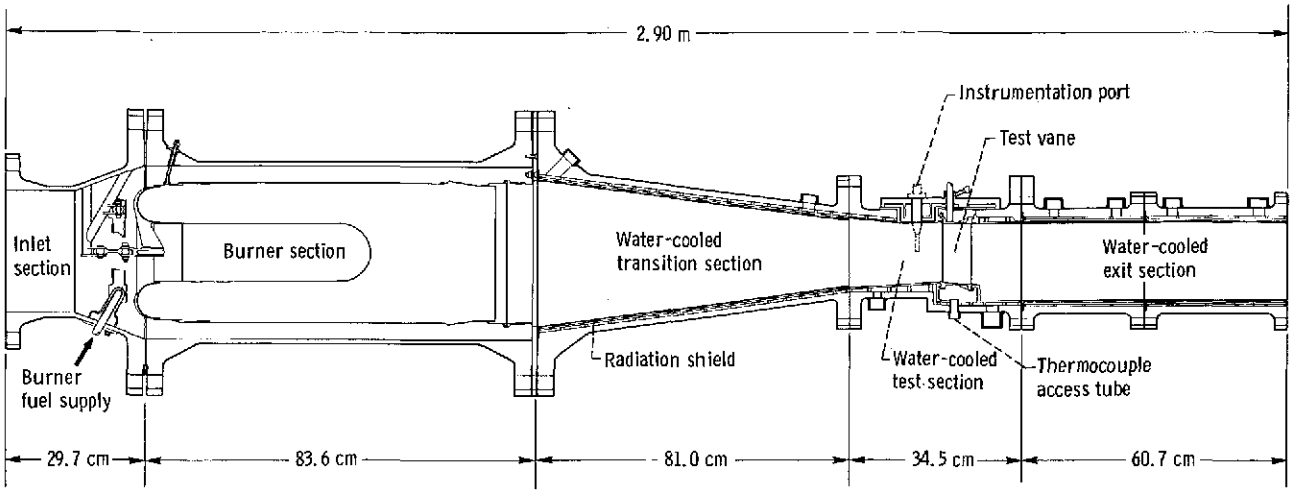

Figure 1. - Schematic cross-sectional view of four-vane cascade facility.

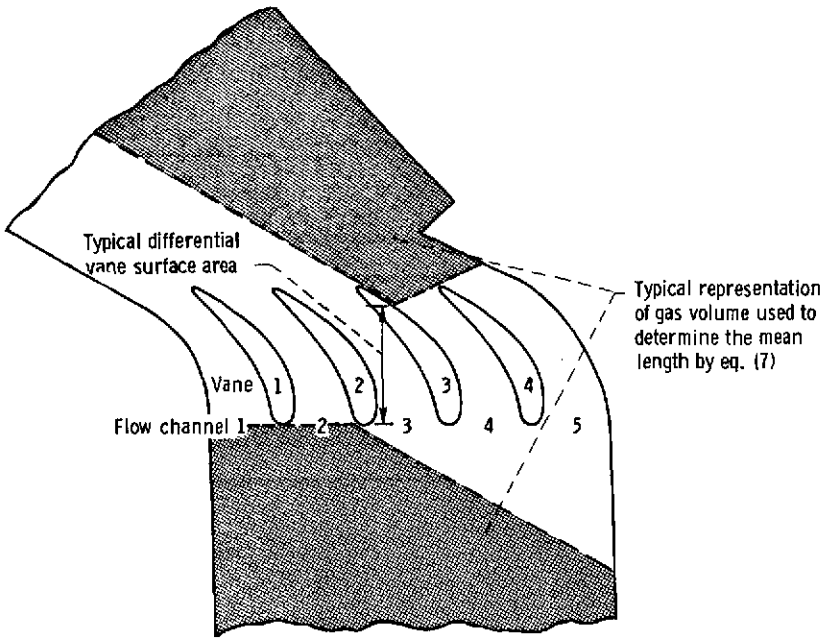

(a) Mean beam length.

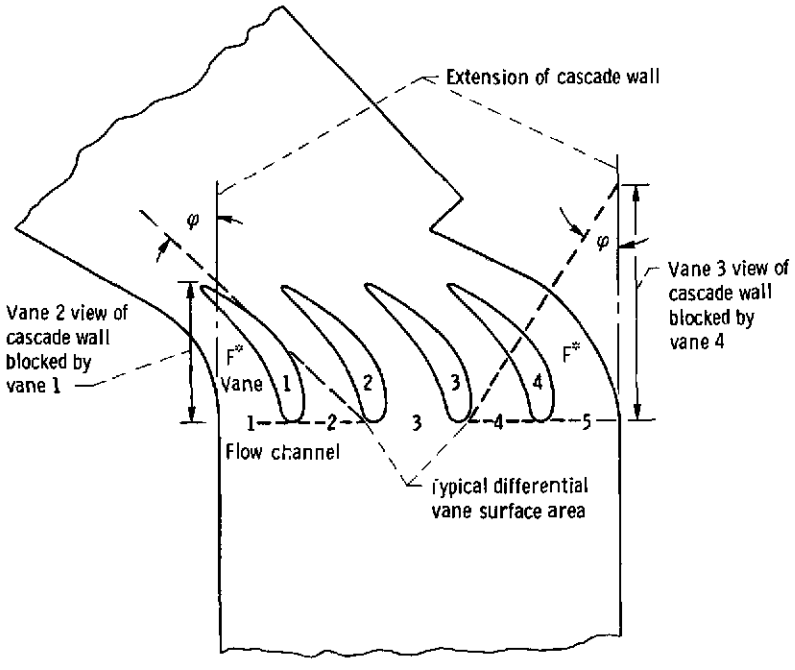

(b) Diffuse view factors.

Figure 2. - Cross-sectional view of vanes and test section showing typical layout used to determine mean beam lengths and diffuse view factors.

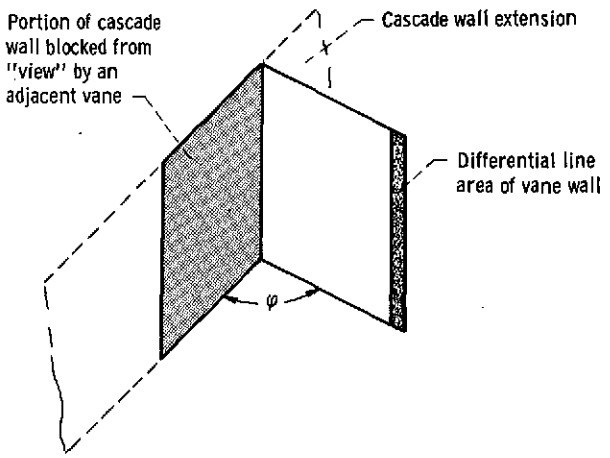

Figure 3. - Configuration for determination of diffuse view factor F^*.

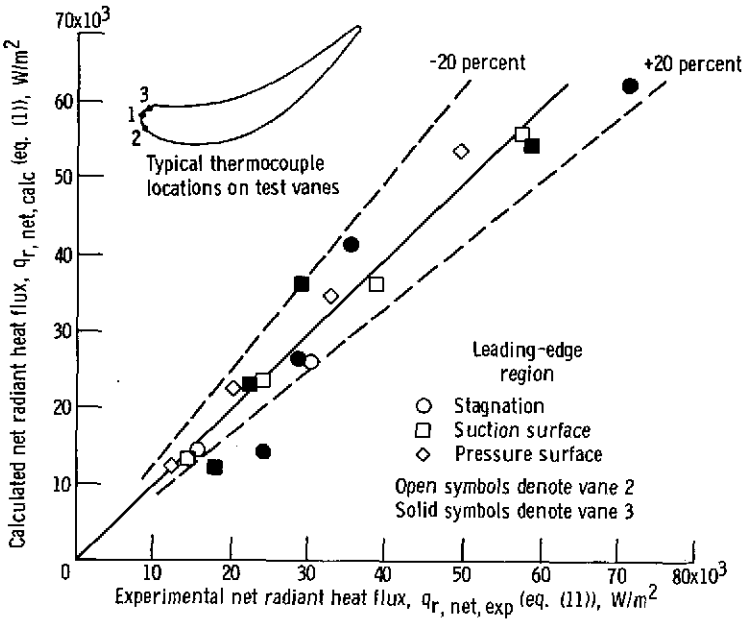

Figure 4. - Comparison of calculated net radiation heat flux and experimental net radiation heat flux from reference 1.

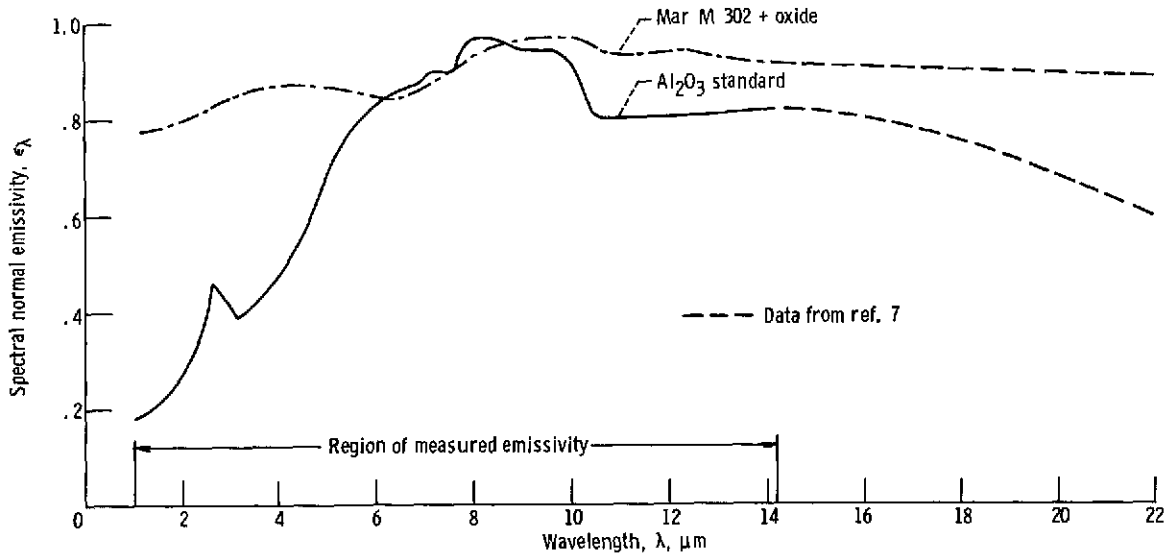

Figure 5. - Spectral normal emissivity of Al_2O_3 and oxidized Mar M-302 at 300 to 1088 K.

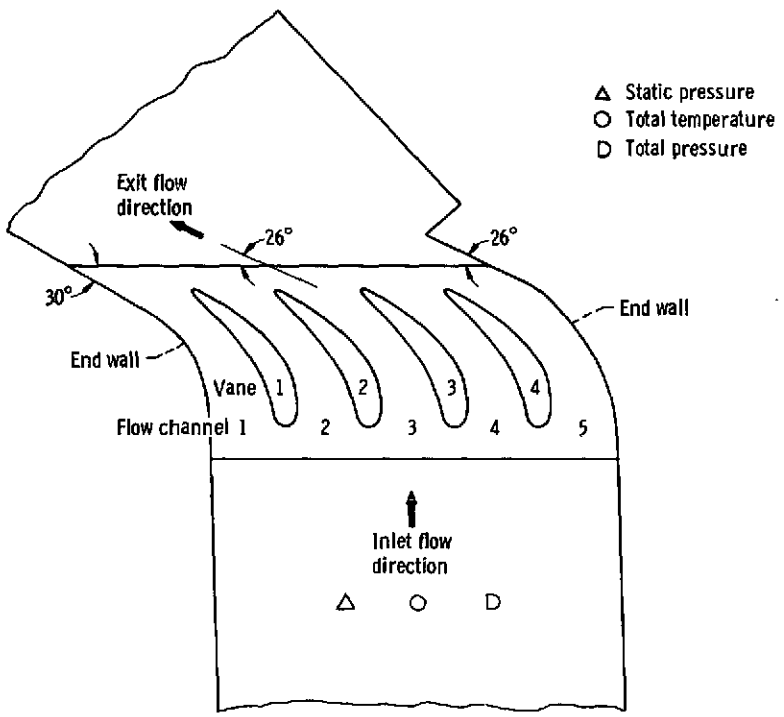

Figure 6. - Plan view of four-vane cascade facility of reference 1.